Amendments to the Drawings:

The attached sheet of drawings, marked as **"Replacement sheet"**, include a change to Figure 4, as set forth in the accompanying remarks.

This Replacement sheet, which includes Figures 4 and 5, is intended to replace the objected drawing sheet including Figures 4 and 5.

A marked-up copy of the amended figure showing the changes made is also enclosed, wherein the modification is encircled for easy identification.

Remarks

Reconsideration of the application as hereby amended, in response to the Examiner's objections, is respectfully requested.

In compliance with the Examiner's request, a copy of the relevant pages 292-297 and 444- 447 from *Modern Optical Engineering-The Design of the Optical Systems by Smith J. Warren (second edition) Mc.Graw-Hill, New York (1990),* is herewith provided as a factual evidence of the applicant's previous statements.

The Examiner's observation and related objection for the non-compliance of the amendment of Figure 4 showing the distance E, submitted with the applicant's letter of April 1, 2005, with the description and claims is correct and founded .

Applicant apologizes for the unintentional error and submits herewith a new amended Figure 4, in which the distance E is correctly indicated as between the eye of the driver and the point O on face 14 of the mirror (see also specification page 5, lines 15-17 and Figure 3.

The terminology of Claims 10 and 19 deemed unclear has been amended to correspond to the statement of the specification, at page 8, lines 7-10).

It is unambiguously derivable for those skilled in the art that the distance E (and magnification M) are selected in accordance with the dimensions and type of the car and as provided also in the pertinent standards, this being usual and known in the art (see US 4 449 786 column 4 lines 14-15 and claim 1, lines 54-56, and Standard No. 111 § 571.111, 49CFR Ch. V (10-1-01 Edition).

Therefore, it is now believed that the application is in an allowable form.

It will be noted that a sincere effort has been made to positively respond to all of

the points raised by the Examiner.

Favorable action by allowance of the application is respectfully solicited.

While it is believed that the amended claims properly and clearly define the present invention, applicant would be open to any suggestion or amendment the Examiner may have or propose concerning different claim phraseology which, in the Examiner's opinion, more accurately defines the present invention.

Respectfully submitted

Albert Josif (Reg. No. 22,917)
Agent for the applicant

Date:	October 6, 2005
Address:	Via Meravigli 16, 20123 MILAN-ITALY
Telephone:	(from USA) (011)(39)(02)8590-7777
Telefax:	(from USA)(011)(39)(02)863-860

Encl.: - sheet of drawings, marked as "Replacement sheet", showing Figures 4 and 5;
- marked-up copy of the amended figure 4;
- copy of the relevant pages 292-297 and 444- 447 from *Modern Optical Engineering-The Design of the Optical Systems by Smith J. Warren (second edition) Mc.Graw-Hill, New York (1990).*

Example B—Skew Trace through a Sphere

	Object Plane	First Surface	Second Surface	Image Plane
R		+ 50	− 50	
c	0.0	+ 0.02	− 0.02	0.0
t	+ 200.	+ 15.	+ 65.517241	
N	1.0	1.50	1.0	
Transfer:				
e by 10.3c		+ 199.989898	+ 12.188013	+ 71.880665
M_1 by 10.3d		− 2.0201051	+ 1.590643	− 8.468077
M^2 by 10.3e		+ 404.040416	+ 389.289720	+ 107.475746
E by 10.3f		+ 0.9586247	+ 0.8772472	+ 0.9224280
L by 10.3g		+ 208.546141	+ 6.327736	+ 75.820392
x by 10.3h	(0.0)	+ 4.470247	− 4.237126	0.000000
y by 10.3i	(+20.0)	− 0.654614	− 1.046081	− 7.078810
z by 10.3j	(0.0)	+ 20.654614	+ 20.116291	− 8.456088
Refraction:				
E' by 10.3k		+ 0.9398771	+ 0.6839135	
g by 10.3l		+ 0.3673232	− 0.6219573	
X by 10.3m	(+0.9899495)	+ 0.9944627	+ 0.9224280	
Y by 10.3n	(−0.1)	− 0.0616676	− 0.0797745	
Z by 10.3o	(+0.1)	− 0.0850734	− 0.3778396	
Check:				
zero by 10.3a	(0.0)	+ 0.0000001	− 0.0000015	
1.0 by 10.3b	(1.0)	1.0000000	1.0000001	

10.5 General, or Skew, Rays: Aspheric Surfaces

For raytracing purposes, an aspheric surface of rotation is conveniently represented by an equation of the form

$$x = f(y, z) = \frac{cs^2}{[1 + \sqrt{1 - c^2s^2}]} + A_2s^2 + A_4s^4 + \cdots + A_js^j \qquad (10.4a)$$

where x is the longitudinal coordinate (abscissa) of a point on the surface which is a distance s from the x-axis. Using the same coordinate system as Section 10.4, the distance s is related to coordinates y and z by

$$s^2 = y^2 + z^2 \qquad (10.4b)$$

As shown in Fig. 10.5, the first term of the right-hand side of Eq. 10.4a is the equation for a spherical surface of radius $R = 1/c$. The subsequent terms represent deformations to the spherical surface, with A_2, A_4, etc., as the constants of the second, fourth, etc., power deformation terms. Since any number of deformation terms may be included, Eq.

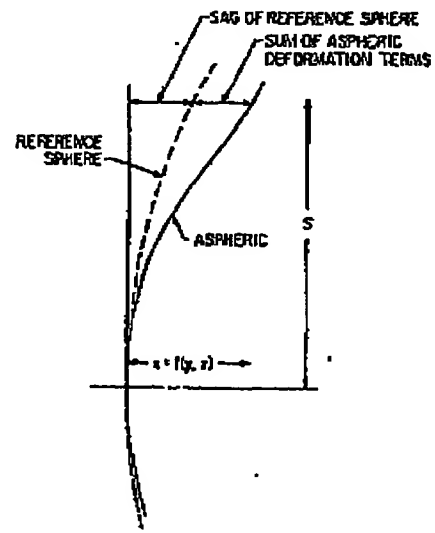

Figure 10.5 Showing the significance of Equation 10.4a, which defines an aspheric surface by a deformation from a reference spherical surface. The x coordinate of a point on the surface is the sum of the x coordinate of the reference sphere and the sum of all the deformation terms.

10.4a is quite flexible and can represent some rather extreme aspherics. Note that Eq. 10.4a is redundant in that the second-order deformation term (A_2s^2) is not necessary to specify the surface, since it can be implicitly included in the curvature c. The importance of the inclusion of this term is that otherwise a large value of c (i.e., a short radius) could be required to describe the surface, and rays which would actually intersect the aspheric surface might not intersect the reference sphere. As can be seen from Example C, if necessary the reference sphere may be a plane.

Aspheric surfaces which are *conic sections* (paraboloid, ellipsoid, hyperboloid) can be represented by a power series; see Section 13.5 for further details.

The difficulty in tracing a ray through an aspheric surface lies in determining the point of intersection of the ray with the aspheric, since this cannot be determined directly. In the method given here, this is accomplished by a series of approximations, which are continued until the error in the approximation is negligible.

The first step is to compute x_0, y_0, and z_0, the intersection coordinates of the ray with the spherical surface (of curvature c) which is usually a fair approximation to the aspheric surface. This is done with Eqs. 10.3c through 10.3j of the preceding section.

Then the x coordinate of the aspheric ($\bar{x}_0$) corresponding to this dis-

tance from the axis is found by substituting $s_0^2 = y_0^2 + z_0^2$ into the equation for the aspheric (10.4a)

$$\bar{x}_0 = f(y_0, z_0) \tag{10.4c}$$

Then compute

$$l_0 = \sqrt{1 - c^2 s_0^2} \tag{10.4d}$$

$$m_0 = -y_0[c + l_0(2A_2 + 4A_4 s_0^2 + \cdots + jA_j s_0^{(j-2)})] \tag{10.4e}$$

$$n_0 = -z_0[c + l_0(2A_2 + 4A_4 s_0^2 + \cdots + jA_j s_0^{(j-2)})] \tag{10.4f}$$

$$G_0 = \frac{l_0(\bar{x}_0 - x_0)}{(Xl_0 + Ym_0 + Zn_0)} \tag{10.4g}$$

where X, Y, and Z are the direction cosines of the incident ray.

Now an improved approximation to the intersection coordinates is given by

$$x_1 = G_0 X + x_0 \tag{10.4h}$$

$$y_1 = G_0 Y + y_0 \tag{10.4i}$$

$$z_1 = G_0 Z + z_0 \tag{10.4j}$$

The process is sketched in Fig. 10.6.

The approximation process is now repeated (from Eq. 10.4c to 10.4j)

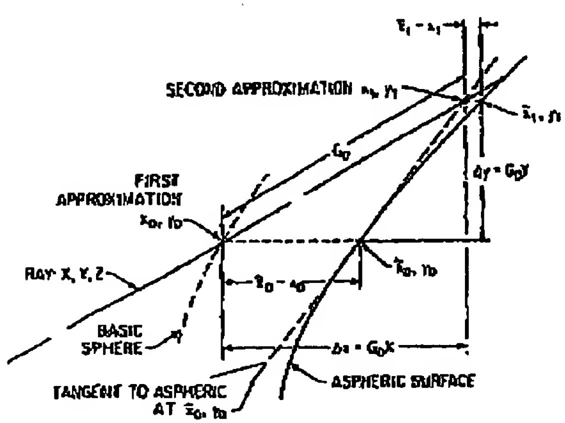

Figure 10.6 Determination of the ray intersection with an aspheric surface. The intersection is found by a convergent series of approximations. Shown here are the relationships involved in finding the first approximation after the intersection with the basic reference sphere has been determined.

until the error is negligible, i.e., until (after k times through the process)

$$x_k = \bar{x}_k \tag{10.4k}$$

to within sufficient accuracy for the purposes of the computation.

The refraction at the surface is carried through with the following equations:

$$P^2 = l_k^2 + m_k^2 + n_k^2 \tag{10.4l}$$

$$F = Xl_k + Ym_k + Zn_k \tag{10.4m}$$

$$F' = \sqrt{P^2\left(1 - \frac{N^2}{N_1^2}\right) + \frac{N^2}{N_1^2}F^2} \tag{10.4n}$$

$$g = \frac{1}{P^2}\left(F' - \frac{N}{N_1}F\right) \tag{10.4o}$$

$$X_1 = \frac{N}{N_1}X + gl_k \tag{10.4p}$$

$$Y_1 = \frac{N}{N_1}Y + gm_k \tag{10.4q}$$

$$Z_1 = \frac{N}{N_1}Z + gn_k \tag{10.4r}$$

This completes the trace through the aspheric. The spatial intersection coordinates are x_k, y_k, and z_k, and the new direction cosines are X_1, Y_1, and Z_1.

Example C

As a numerical example, let us trace the path of a ray through a paraboloidal mirror. The equation of a paraboloid with vertex at the origin is

$$x = \frac{s^2}{4f}$$

and if we choose a concave mirror with a focal length of −5, the constants of Eq. 10.4a become $c = 0$, $A_2 = 1/4f = -0.05$, and A_4, A_6, etc., equal zero. Thus

$$x = -0.05s^2 = -0.05(y^2 + z^2)$$

We will place the initial reference plane at the vertex of the parabola and the final reference (image) plane at the focal point. Thus $t = 0$

and $t_1 = f = -5$ (following our usual sign convention for distance after reflections). We will trace the ray striking the reference plane at $x = 0, y = 0, z = 1.0$ at a direction of $Y = 0.1, Z = 0$, and (by Eq. 10.3b) $X = 0.9949874$. The index of refraction before reflection N equals 1.0 and the index after reflection N_1 will then be -1.0, again following the convention of reversed signs after reflection.

The computation is indicated in the following tabulation, where the applicable equation number is given in parentheses at each step. The steps indicated by (10.4d) through (10.4c) are repeated top to bottom until $\bar{x}_1 = x_1$ to (in this instance) seven places past the decimal. The fact that this example converged in only two cycles despite the fact that $c = 0$ is a poor approximation to our paraboloid, is an indication of the rapidity of convergence of this technique.

Reference surface: $c_0 = 0 \quad t_0 = 0.0 \quad N_0 = 1.0$

Aspheric: $x = -0.05s^2 \quad c_1 = 0 \quad A_2 = -0.05 (A_4$, etc. $= 0)$

$t_1 = -5.0 \quad N_1 = -1.0$

Image surface: $c_2 = 0$

Given: $x = 0, y = 0, z = +1.0$

$X = +0.9949874 \quad Y = +0.10 \quad Z = 0.0$

Since $c = 0$ for the aspheric, it is obvious that $x_0 = x = 0, y_0 = y = 0$, and $z_0 = z = 1.0$. Thus, $\bar{x}_0 = -0.05(y^2 + z^2) = -0.05$ (by Eq. 104c) and $\bar{x}_0 - x_0 = -0.05$. (The same results can be obtained from Eqs. 10.3c through j)

Intersection of Ray with Aspheric:

(10.4d)	$l_0 = +1.0$	$l_1 = +1.0$
(10.4e)	$m_0 = 0.0$	$m_1 = -0.0005025$
(10.4f)	$n_0 = +0.1$	$n_1 = +0.1$
(10.4g)	$G_0 = -0.0502519$	$G_1 = -0.0000013$
(10.4h)	$x_1 = -0.050$	$x_2 = -0.0500013$
(10.4i)	$y_1 = -0.0050252$	$y_2 = -0.0050258$
(10.4j)	$z_1 = +1.0$	$z_2 = +1.0$
(10.4c)	$\bar{x}_1 = -0.0500013$	$\bar{x}_2 = -0.0500013$
	$\bar{x}_1 - x_1 = -0.0000013$	$\bar{x}_2 - x_2 = 0.0000000$

Refraction:

(10.4l)	$P^2 = +1.0100002$
(10.4m)	$F = +0.9949372$
(10.4n)	$F' = +0.9949372$
(10.4o)	$g = +1.9701722$
(10.4p)	$X_1 = +0.9751848$
(10.4q)	$X_1 = -0.1009900$
(10.4r)	$Z_1 = +0.1970172$
	$X_1^2 + Y_1^2 + Z_1^2 = 1.0000001$

Intersection of Ray with Image Surface:

(10.3c)	$e_1 = -5.0248880$
(10.3d)	$M_{2L} = +0.0499993$
(10.3e)	$M_2^2 = +0.2550229$
(10.3f)	$E_2 = +0.9751848$
(10.3g)	$L_1 = -5.0769596$
(10.3h)	$x_2 = 0$
(10.3i)	$y_2 = +0.5075959$
(10.3j)	$z_2 = -0.0000613$

10.6 Coddington's Equations

The tangential and sagittal curvature of field can be determined by a process which is equivalent to tracing paraxial rays along a principal ray, instead of along the axis. In Chapter 3, it was pointed out that the slope of the ray intercept plot was equal to X_t, the tangential field curvature. This slope *could* be determined by tracing two closely spaced meridional rays and computing

$$X_t = \frac{H'_1 - H'_2}{\tan U'_2 - \tan U'_1} = \frac{-\Delta H'}{\Delta \tan U'}$$

and a similar process using close sagittal (skew) rays would yield X_s, the sagittal field curvature.

Coddington's equations are equivalent to tracing a pair of infinitely

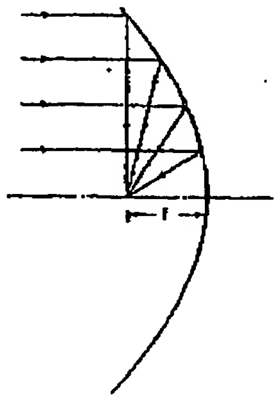

Figure 13.40 Illustrating the extreme variation of focal length with ray height in an f/0.25 parabolic reflector.

ation of magnification with aperture"). The parabola is thus aberration-free only *exactly* on the axis.

The apparent contradiction of our image illumination principles is thus resolved since we had assumed aplanatic systems in their derivations. From another viewpoint, we can remember that although the parabola forms a perfect image of an infinitesimal (geometrical) point, such a point (being infinitesimal) cannot emit a real amount of energy; the moment one increases the object size to any real dimension, the parabola has a real field, the image becomes comatic, and the energy in the image is spread out over a finite blur spot. This reduces the image illumination to that indicated as the maximum in Chapter 8.

The Cassegrain objective system is used (usually in a modified form) in a great variety of applications because of its compactness and the fact that the second reflection places the image behind the primary mirror where it is readily accessible. It suffers from a very serious drawback when an appreciable field of view is required, in that an extreme amount of baffling is necessary to prevent stray radiation from flooding the image area. Figure 13.41 indicates this difficulty and the type of baffles frequently used to overcome this problem. An exterior

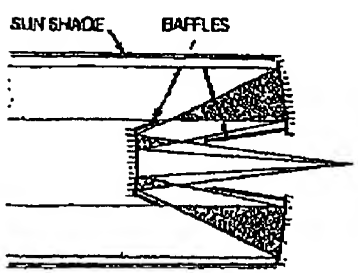

Figure 13.41 Complex conical baffles are necessary in a Cassegrain objective to prevent stray radiation from flooding the image plane.

"sunshade," which is an extension of the main exterior tube of the scope, is frequently used in addition to the internal baffles.

Because of their uniaxial character, aspheric surfaces are much more difficult to fabricate than ordinary spherical surfaces. A strong paraboloid may cost an order of magnitude more than the equivalent sphere; ellipsoids and hyperboloids are a bit more difficult, and nonconic aspherics are more difficult still. Thus one might well think twice (or three times) before specifying an aspheric. Often a spherical system can be found which will do nearly as well at a fraction of the cost. This is also true in refracting systems of moderate size where several ordinary spherical elements can be purchased for the cost of a single aspheric. For very large one-of-a-kind systems, however, aspherics are frequently a sound choice. This is because the large systems (e.g., astronomical objectives) are, in the final analysis, handmade, and the aspheric surface adds only a little to the optician's task.

Conic section through the origin. Where r is the radius (at the axis) and c is the curvature ($c = 1/r$)

$$y^2 - 2rx + px^2 = 0$$

$$x = \frac{r \pm \sqrt{r^2 - py^2}}{p} = \frac{cy^2}{1 + \sqrt{1 - pc^2y^2}}$$

$$x = \frac{y^2}{2r} + \frac{1py^4}{2^2 2! r^3} + \frac{1 \cdot 3 p^2 y^6}{2^3 3! r^5} + \frac{1 \cdot 3 \cdot 5 p^3 y^8}{2^4 4! r^7} + \frac{1 \cdot 3 \cdot 5 \cdot 7 p^4 y^{10}}{2^5 5! r^9} + \cdots$$

Ellipse	$p > 1$	conic constant Kappa $= p - 1$
Circle	$p = 1$	conic eccentricity $e = \sqrt{1 - p}$
Ellipse	$1 > p > 0$	
Parabola	$p = 0$	
Hyperbola	$p < 0$	

Distance to foci: $\frac{r}{p}(1 \pm \sqrt{1 - p})$

Magnification: $-\left[\frac{1 + \sqrt{1 - p}}{1 - \sqrt{1 - p}}\right]$

Intersects axis at: $x = 0, \frac{2r}{p}$

Distance between conic and a circle of the same vertex radius r (i.e.,

departure from a sphere):

$$\Delta x = \frac{(p-1)y^4}{2^2 2!\, r^3} + \frac{1\cdot 3\,(p^2-1)y^6}{2^3 3!\, r^5} + \frac{1\cdot 3\cdot 5\,(p^3-1)y^8}{2^4 4!\, r^7} + \cdots$$

Angle between the normal to the conic and the x-axis:

$$\phi = \tan^{-1}\left[\frac{-y}{(r-px)}\right]$$

$$\sin\phi = \frac{-y}{[y^2+(r-px)^2]^{1/2}}$$

Radius of curvature:

Meridional: $$R_t = \frac{R_s^3}{r^2} = \frac{[y^2+(r-px)^2]^{3/2}}{r^2}$$

Sagittal (distance to axis along normal):

$$R_s = [y^2+(r-px)^2]^{1/2}$$

The Schmidt system. The Schmidt objective (Fig. 13.42) can be viewed as an attempt to combine the wide uniform image field of the stop-at-the-center sphere with the "perfect" imagery of the paraboloid. In the Schmidt, the reflector is a sphere and the spherical aberration is corrected by a thin refracting aspheric plate at the center of curvature. Thus the concentric character of the sphere is preserved in great measure, while the spherical aberration is completely eliminated (at least for one wavelength).

The aberrations remaining are chromatic variation of spherical aberration and certain higher-order forms of astigmatism or oblique spherical which result from the fact that the off-axis ray bundles do

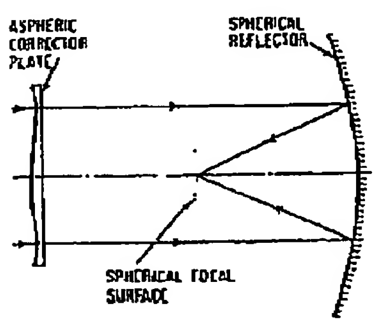

Figure 13.42 The Schmidt system consists of a spherical reflector with an aspheric corrector plate at its center of curvature. The aspheric surface in the f/1 system shown here is greatly exaggerated.

not strike the corrector at the same angle as do the on-axis bundles. The action of a given zone of the corrector is analogous to that of a thin refracting prism. For the axial bundle, the prism is near minimum deviation; as the angle of incidence changes, the deviation of the "prism" is increased, introducing overcorrected spherical. Since the action is different in the tangential plane than in the sagittal plane, astigmatism results. This combination is oblique spherical aberration. The meridional angular blur of a Schmidt system is well approximated by the expression

$$\beta = \frac{u_p^2}{48(f/\#)^3}\ \text{radians} \qquad (13.23)$$

There are obviously an infinite number of aspheric surfaces which may be used on the corrector plate. If the focus is maintained at the paraxial focus of the mirror, the *paraxial* power of the corrector is zero and it takes the form of a weak concave surface. The best forms have the shape indicated in Fig. 13.42, with a convex paraxial region and the minimum thickness at the 0.866 or 0.707 zone, depending on whether it is desired to minimize chromatic aberration or to minimize the material to be ground away in fabrication. The performance of the Schmidt can be improved slightly by (1) incompletely correcting the axial spherical to compensate for the off-axis overcorrection, (2) "bending" the corrector slightly, (3) reducing the spacing, (4) using a slightly aspheric primary to reduce the load on, and thus the overcorrection introduced by, the corrector. Further improvements have been made by using more than one corrector and by using an achromatized corrector.

A near-optimum corrector plate has a surface shape given by the equation

$$x = 0.5Cy^2 + Ky^4 + Ly^6$$

where

$$C = \frac{3}{128(N-1)f(f/\#)^2}$$

$$K = \frac{[1 - 3/64(f/\#)^2]^2}{32(1-N)f^3}$$

$$L = \frac{1}{85.8(1-N)f^5}$$

The aspheric corrector of the Schmidt is usually easier to fabricate than is the aspheric surface of the paraboloid reflector. This is because

ANNOTATED MARKED-UP DRAWING

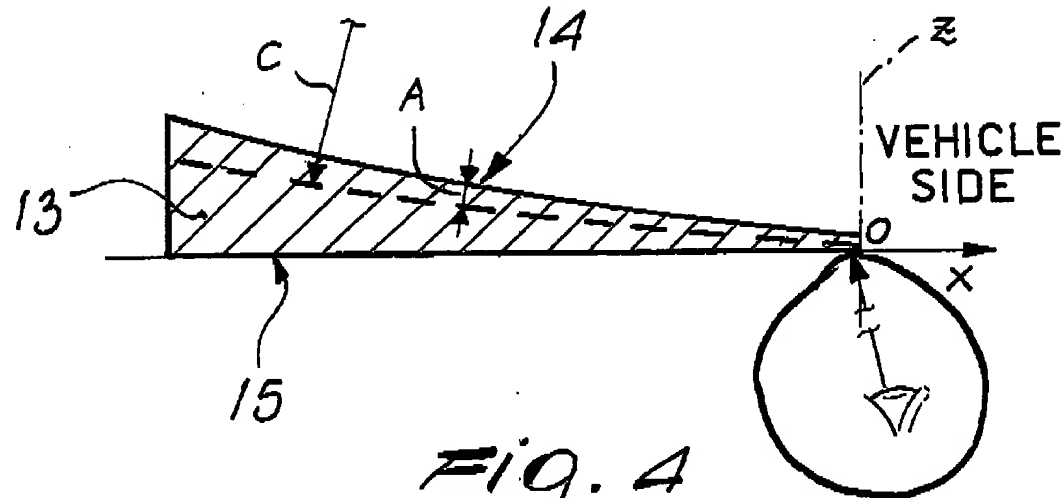

Fig. 4

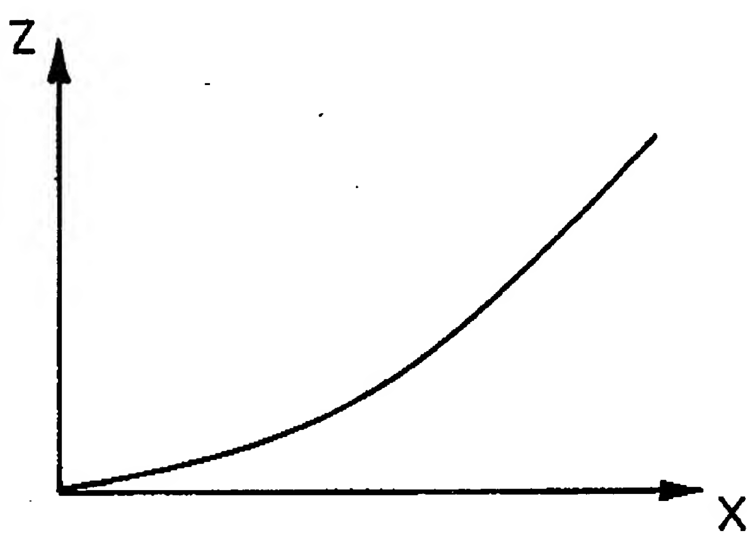

Fig. 5